APL Materials

Theoretical calculation boosting the chemical vapor deposition growth of graphene film

Cite as: APL Mater. **9**, 060906 (2021); https://doi.org/10.1063/5.0051847
Submitted: 28 March 2021 . Accepted: 02 June 2021 . Published Online: 15 June 2021

Ting Cheng, Luzhao Sun, Zhirong Liu, Feng Ding, Zhongfan Liu, et al.

Theoretical calculation boosting the chemical vapor deposition growth of graphene film

Cite as: APL Mater. 9, 060906 (2021); doi: 10.1063/5.0051847
Submitted: 28 March 2021 • Accepted: 2 June 2021 •
Published Online: 15 June 2021

Ting Cheng,[1,2] Luzhao Sun,[1,2] Zhirong Liu,[1] Feng Ding,[3,4,a)] and Zhongfan Liu[1,2,a)]

AFFILIATIONS

[1] Center for Nanochemistry, Beijing Science and Engineering Center for Nanocarbons, Beijing National Laboratory for Molecular Sciences, Academy for Advanced Interdisciplinary Studies, College of Chemistry and Molecular Engineering, Peking University, Beijing 100871, China
[2] Beijing Graphene Institute (BGI), Beijing 100095, China
[3] Centre for Multidimensional Carbon Materials, Institute for Basic Science, Ulsan, South Korea
[4] School of Materials Science and Engineering, Ulsan National Institute of Science and Technology, Ulsan, South Korea

Note: This paper is part of the Special Topic on 2D Materials Chemistry.
[a)] **Authors to whom correspondence should be addressed:** f.ding@unist.ac.kr and zfliu@pku.edu.cn

ABSTRACT

Chemical vapor deposition (CVD) is a promising method for the mass production of high-quality graphene films, and great progress has been made over the last decade. Currently, the CVD growth of graphene is being pushed to achieve further advancements, such as super-clean, ultra-flat, and defect-free materials, as well as controlling the layer, stacking order, and doping level during large-scale preparation. The production of high-quality graphene by CVD relies on an in-depth knowledge of the growth mechanisms, in which theoretical calculations play a crucial role in providing valuable insights into the energy-, time-, and scale-dependent processes occurring during high-temperature growth. Here, we focus on the theoretical calculations and discuss the recent progress and challenges that need to be overcome to achieve controllable growth of high-quality graphene films on transition-metal substrates. Furthermore, we present some state-of-the-art graphene-related structures with novel properties, which are expected to enable new applications of graphene-based materials.

INTRODUCTION

Graphene, which is composed of sp^2-bonded carbon atoms, continues to attract widespread interest from academia and industry and has triggered the development of the entire field of two-dimensional materials. The controllable synthesis of such materials is the foundation of their applicability in various fields. Chemical vapor deposition (CVD), which is a widely used bottom-up synthesis approach in the semiconductor industry, is considered the most promising method to realize the mass production of high-quality graphene films.[1,2] In particular, graphene films grown on catalytic transition-metal substrates now have excellent properties, which are comparable to those of mechanically exfoliated graphene.[3,4] In the last decade, tremendous improvements were made in this field, such as increasing the size and growth rate of single-crystal graphene (SCG)[5–12] and the successful preparation of wrinkle-free graphene, super-clean graphene, and large-area bilayer and trilayer graphene.[3,8,13–22] In addition, various models for the controllable growth of graphene have been developed, which have helped clarify the related mechanisms. CVD processes usually operate at high temperatures (~1000 °C) and under vacuum, which makes it difficult to directly observe the deposition process and the growth of graphene at the nanometer scale. Fortunately, theoretical calculations can provide insight into the energy of the system via the thermodynamics and kinetics, as well as an understanding of the high-temperature reaction processes during CVD, and are expected to contribute to further experimental advancements.[23–31]

Here, we focus on theoretical calculations used to enhance the controllable growth of high-quality graphene films via the CVD method. First, we provide a brief introduction of multiscale calculations and outline recent achievements in van der Waals epitaxial growth of SCG. Then, two key issues affecting the quality of graphene films (surface contamination and roughness) are discussed. In addition, new graphene-related structures, which can be

achieved by controlling the number of layers, stacking order, and doping of the graphene, are discussed as they are expected to display novel properties. The recent progress is analyzed and placed in context by discussing the major challenges in the field and future perspectives.

MULTI-SCALE CALCULATIONS OF GRAPHENE GROWTH

Figure 1 presents several theoretical calculation methods for the modeling and simulation of graphene growth, which have been classified by both the time and length scales over which they can be used.

The density functional theory (DFT) approach (also called the *ab initio* method) is within the framework of quantum mechanics and Kohn–Sham equations.[32–37] Information such as the stability, formation energy of the system, and the energy barrier of the chemical reaction all originate from the Schrodinger equation, which is further converted to the more easily solvable Kohn–Sham equation. Consequently, DFT calculations have relatively high accuracy and can reliably predict various useful physical quantities, becoming one of the most widely used computational methods. Using

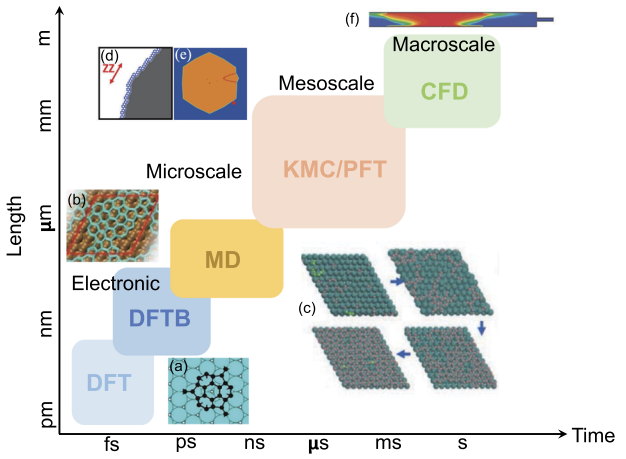

FIG. 1. Major theoretical calculation methods used for the modeling and simulation of graphene growth, classified by the length and time scales. (a) Examples of a magic carbon cluster observed in graphene CVD growth on Ru(0001) and Rh(111) surfaces with the DFT method. Reproduced with permission from Gao *et al.*, Angew. Chem. Int. Ed. **126**, 14255 (2014). Copyright 2014 Wiley-VCH.[60] (b) Snapshots of the simulated carbon network grown from coronene on a template on the Ni(111) terrace via 50 ps DFTB/MD simulation. Reproduced with permission from Wang *et al.*, J. Am. Chem. Soc. **133**, 18837 (2011). Copyright 2011 American Chemical Society.[61] (c) Snapshots taken from the trajectory of graphene growth on the Ni(111) surface via MD simulation. (d) Atomic edge structures of a graphene island in KMC simulation. Reproduced with permission from Kong *et al.*, npj Comput. Mater. **7**, 14 (2021). Copyright 2021 Springer Nature.[56] (e) PFT simulation showing the formation process of a graphene island through coalescence with a small graphene grain around it. Reproduced with permission from Dong *et al.*, Angew. Chem. Int. Ed. **58**, 7723 (2019). Copyright 2019 American Chemical Society.[51] (f) Contours of molar concentration of methane distribution on the symmetry plane at low-pressure CVD with a simulating temperature of 1270 K. Reproduced with permission from Li *et al.*, Phys. Chem. Chem. Phys. **17**, 22832 (2015). Copyright 2015 Royal Society of Chemistry.[59]

DFT calculations, the energy barriers of CH_4 dissociation on Cu and other transition metal surfaces were determined, thereby revealing the corresponding dissociation processes.[38,39] Subsequently, a comprehensive DFT study of the absorption and diffusion barriers of various active carbon species on four representative metal surfaces, Cu(111), Ni(111), Ir(111), and Rh(111), was performed.[40] Based on these energy barriers, the thermodynamics and kinetics of graphene growth can be determined using various equations, most of which are variants of the Arrhenius equation $k = Ae^{-\frac{E_a}{RT}}$, where k is the reaction rate, E_a is the energy, T is the temperature, and R is the universal gas constant.

However, the time scale (fs) and length scale (nm) of the DFT approach are far from those used in the practical CVD growth process of graphene. In addition, DFT calculations usually provide only the information at 0 K (ground state), which is distinct from the experimental conditions (1000–1300 K). Therefore, factors such as the vibration of atoms are usually considered to incorporate the effects of temperature. In contrast, molecular dynamics (MD) simulations are within the framework of classic Newtonian mechanics; thus, the timescale can reach nanoseconds and the length scale can reach up to hundreds of nanometers. MD simulations model ensembles of particles in liquid, solid, or gaseous states, providing a view of the dynamic evolution of the system, including temperature effects.[41–43] Very recently, based on the self-developed Cu–C potential, the graphene sinking process on a semi-molten Cu surface during CVD growth was simulated.[44] However, the accuracy of the MD method depends significantly on the classic force field potential, which requires a huge parameterization effort to achieve results close to those from DFT methods. In addition, insufficient simulation time mostly leads to defective graphene islands.

Finite-temperature density functional theory based-molecular dynamics (DFT-MD) combines the force calculated from DFT with some classic MD component. The timescale can be increased to the picosecond scale, although the computational burden of DFT-MD is heavy and the number of atoms in the system is limited to hundreds.[45,46] The DFT-based tight binding (DFTB) method and its extension (DFTB+) offer an alternative tool, enabling simulations of larger systems (hundreds of nanometers) and longer timescales (ps) with reasonable accuracy.[47–50]

Kinetic Monte Carlo (KMC) and phase field theory (PFT) methods can allow for the analysis of larger systems (up to tens of micrometers), over a longer timescale (typically microseconds and beyond), than the previously discussed methods. For instance, PFT has often been used to explore the morphological evolution of graphene islands and polycrystalline grain growth resulting from a concentration gradient and flux of species or growth dynamics.[5,7,51,52] Moreover, the predicted results can be directly compared with experiments with good consistency of the time and length scales. Although PFT lacks the details of the atomic structure, KMC can compensate for this shortcoming. KMC, typically rejection-KMC, is often used to simulate graphene growth processes that occur with all the key transition rates among states.[53–56] Accordingly, it is important to fully understand these rates as inputs for the KMC model, which strongly influences the shape and growth rate of graphene islands. Generally, these kinetic parameters are obtained from DFT calculations by identifying the minimum energy path

(MEP). However, such a MEP-based protocol is questionable when describing high-temperature reactions, while the DFT-MD method could give a more accurate barrier as inputs for the KMC model.[57] Recently, Kong *et al.* developed a low-computational-cost large-scale KMC algorithm including all possible events of carbon attachment and detachment on various graphene edge sites to reveal a complementary graphene growth and etching process with a single CPU core.[56] This model was able to reproduce experimentally observed shape evolution and provides insight into the physical meaning of each step in the process.

Based on analyzing and solving numerical equations, the computational fluid dynamics (CFD) method makes it possible to study the CVD process on a macroscale (~m in length, ~min/h in time). For example, simulations of heat transfer; the flow fields of temperature, velocity, and molar concentration of the carbon precursor; and the surface deposition rate have been developed.[29,58,59] CFD can predict and directly compare the growth environment in the reaction chamber of the CVD system, which is beneficial for designing key components in pilot or production level equipment. However, atomic-scale information is not provided by this method. It is necessary and urgent to establish the relationship between fluid dynamics and elementary steps of graphene growth.

HIGH-QUALITY LARGE-AREA SCG FILMS

The controllable synthesis of large-area SCG films is an essential prerequisite for electronic and optoelectronic devices and their integrations. In the last decade, theoretical calculations have played an important role in realizing this goal via single-nucleus and multi-nuclei approaches.[62] Currently, the synthesis of high-quality graphene films is targeted toward achieving super-clean, ultra-flat, and defect-free signatures, as well as precise large-scale manufacturing. Multiscale calculations are expected to continue to assist researchers in achieving controllable preparation of high-quality graphene films.

van der Waals epitaxial growth of large-area SCG

The strategies for growing SCG can be divided into two approaches: (1) *single-nucleus approach*, which allows a single seed crystal to evolve into a large domain [Fig. 2(b)], and (2) *multi-nuclei approach*, where well-aligned domains from multi-seed crystals are coalesced on a single-crystal metal foil or film substrates [Fig. 2(e)]. The mechanisms underlying these two strategies are revealed through theoretical calculations.

The single-nucleus approach is based on the "edge epitaxy growth" theory, where the orientation of the matured graphene film inherits the orientation of the graphene nucleus [Figs. 2(a) and 2(b)].[63] Hence, a single graphene domain can cross the grain boundary of a substrate, and a polycrystalline catalyst can be used. Accordingly, researchers have investigated the limitation of the active sites or concentration of active carbon species to decrease the nucleation density. However, this is contradictory to the goal of achieving a high growth rate. Cu–Ni alloys have been used to both decrease the nucleation density and increase the growth rate of a single domain as the alloy has more active catalytic sites than a pure Cu surface.[6,9] DFT calculations revealed that the existence of Ni in the substrate

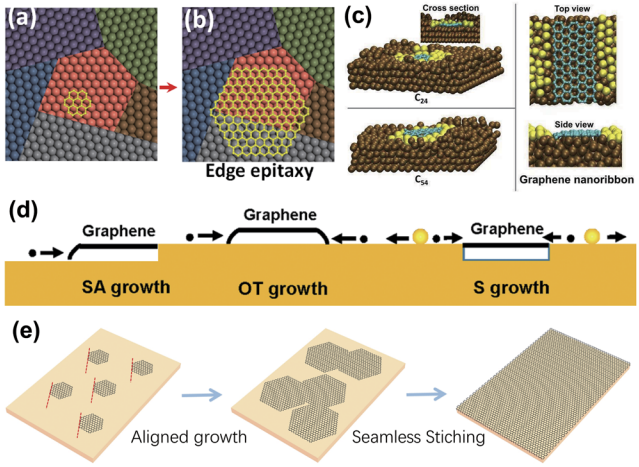

FIG. 2. Illustrations of SCG growth on transition-metal substrates. [(a) and (b)] Illustration of single-crystal graphene growth on a polycrystalline catalyst surface via the edge epitaxy mechanism. Reproduced with permission from Zhang *et al.*, J. Phys. Chem. Lett. **3**, 2822 (2012). Copyright 2012 American Chemical Society.[63] (c) Molecular dynamics simulation of graphene nanostructures (C_{24}, C_{54}, and nanoribbons) sinking on a semi-molten Cu(111) surface. Reproduced with permission from Xu *et al.*, npj Comput. Mater. **6**, 14 (2020). Copyright 2020 Springer Nature.[44] (d) Illustration of the three growth modes of graphene: the step-attached (SA), on-terrace (OT), and sunk (S) growth modes. Reproduced with permission from Yuan *et al.*, J. Phys. Chem. Lett. **5**, 3093 (2014). Copyright 2014 American Chemical Society.[66] (e) Schematics of epitaxial growth of single-crystal graphene on single-crystal metal substrates. Reproduced with permission from Li *et al.*, Inorg. Chem. Front. **8**, 182 (2020). Copyright 2020 Royal Society of Chemistry.[73]

and O_2 or F_2 in the gas phase significantly lowers the energy barrier for decomposing carbon precursor CH_4, which contributes to increasing the graphene growth rate.[5,7,64,65] In addition, O_2 in the gas phase plays a critical role in altering the edges of graphene from H-terminated to metal-passivated, which promotes the attachment of carbon species to the graphene edges. However, the effect of metals with high catalytic activity (e.g., Ni and Pt) on the edge attachment of carbon species and their lattice incorporation remains to be explored. In addition, the effect of the ultrafast growth rate on the defect density of graphene should be clarified in the near future.

In contrast to the single-nucleus method, the multi-nucleation approach is more efficient and relies on heteroepitaxy theory. However, as a two-dimensional material, there are differences between the epitaxial growth of graphene and traditional heteroepitaxy. Three growth modes on metal surfaces, that is, step-attached (SA), sunk (S), and on-terrace (OT) modes, have been proposed [Fig. 2(d)]. By calculating the formation energy difference between the S and OT modes, Yuan *et al.* found that graphene tends to grow in SA or S modes on Cu(111), Au(111), or Pd(111), which provide strong graphene-edge–catalyst interaction, thereby providing the possibility of fixing the graphene orientation relative to the substrate.[66] Classical MD and DFT-MD simulations can consider the premelting phenomenon of the Cu surface (~1273 K) and explore the size of the graphene nanostructure domains [Fig. 2(c)],[44] which is a step toward experimental graphene growth and will contribute

to the further study of the coalescence of small-angle disorientated graphene.

The key issue in realizing the epitaxial growth of well-aligned graphene is to obtain large-area single-crystal metal substrates with suitable symmetry, lattice constants, and strong graphene–catalyst interactions. In the past few years, great progress has been made in the design and preparation of single-crystal metal substrates, which can be classified as foils or wafers.[8,11,67]

Large single-crystal metal foils with (111) orientation and high-index facets were successfully prepared from commercially available polycrystalline foils by thermal annealing based on anomalous grain growth.[8,20,68,69] The Cu(111) surface, with closest-packed arrangement, has the lowest surface energy compared with other facets and could be produced from a polycrystalline foil if the surface energy is the governing driving force.[68] MD simulation results indicated that the grain surface tends to rotate and flatten toward the (111) orientation, resulting in the disappearance of the stacking faults under the stress-free conditions in a hydrogen-rich environment,[68] where the temperature gradient acts as a driving force for grain-boundary migration.[8] Accordingly, single-crystal metal foils with high-index facets can be prepared under conditions where the strain energy or interfacial energy dominates the formation and growth of anomalous grains.[20,69]

Another route to achieve single-crystal metal substrates is the physical deposition of thin metal films (usually <1 μm) on single-crystal inorganic substrates, among which c-plane sapphire wafers are the most frequently used.[8,70,71] Therefore, the single-crystal metal obtained by this method is usually called a single-crystal metal wafer. However, such epitaxial metal films tend to have twin crystals and there is a risk of dewetting during the graphene CVD process because of the thinness of the metal film. This challenge requires further in-depth research, including calculations or simulations of the metal–sapphire interfacial interactions and the recrystallization process of the metal thin films.

Recently, DFT calculation results have revealed that the symmetry of epitaxial substrates should generally be a subgroup of C_{6v}.[72] This rule expands the range of viable substrate orientations, especially for the vicinal surface of the basal facets. However, the presence of some domains with small misalignment angles and those with 30° angles is still inevitable in large-area graphene, which suggests that the design of a substrate is not enough for fulfilling the epitaxial growth of misorientation-free graphene and that the role of gas-phase reactions still needs to be explored. Thus, further theoretical studies of the formation mechanism and kinetic process of misaligned angle domains should be performed using multiscale computational methods. For instance, MD simulations at the atomic scale can provide more information regarding the growth process, relying on which the high accuracy of the C–Cu–H, C–Cu–Ni, and C–Cu–Ni–H potentials should be developed to provide more theoretical references for the large-scale controllable growth of SCG in experiments.

Toward super-clean graphene

During the high-temperature CVD growth of graphene, carbon precursors and intermediate carbon species in the gas phase are involved in complex side reactions that can lead to the formation of amorphous carbon (contamination) on the graphene surface, which strongly degrade the intrinsic properties of graphene [Fig. 3(a)].[3] With the aim of eliminating such surface contamination, a series of strategies for growing super-clean graphene films were sequentially developed as follows: (i) introducing additional gas-phase metal catalysts to promote the decomposition of large carbon clusters using alternating Cu foil and Cu foam stacks or metal-containing carbon precursors,[2,14] (ii) using cold-wall CVD systems to suppress the gas-phase reactions,[17] and (iii) introducing CO_2 for selective chemical etching or force-engineering lint roller to physically remove surface contamination.[16,74] However, these experimental studies were all focused on the cleanliness of one single graphene domain on a polycrystalline Cu surface. Hence, we propose that improving the cleanliness of SCG on single-crystal metal substrates should also be explored to optimize the intrinsic properties of SCG.

The formation of amorphous carbon is dependent on gas-phase and surface reactions; thus, a combination of the above-mentioned theoretical methods at different scales is vital to fully understand these mechanisms. In addition, considering the existence of dangling bonds or the breaking of the charge distribution on an intrinsic graphene lattice, defects can act as absorption sites for carbon species, resulting in the nucleation of amorphous carbon [Fig. 3(b)].[75] Thus, control of the defect density requires

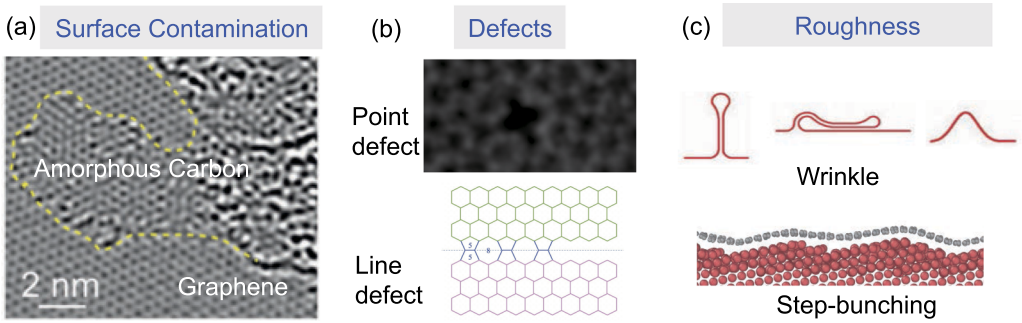

FIG. 3. Key issues affecting the quality of single-crystal graphene. (a) Surface contamination occurring during the high-temperature growth process. Reproduced with permission from Zhang *et al.*, Angew. Chem. Int. Ed. **58**, 14446 (2019). Copyright 2019 Wiley-VCH.[16] (b) Point defects and line defects, which could serve as adsorption sites, leading to the formation of surface contamination. Reproduced with permission from Zheng *et al.*, Nat. Commun. **11**, 8 (2020). Copyright 2020 Springer Nature.[76] (c) Increase in the roughness of the graphene films during the cooling process.

more detailed research. Furthermore, establishing a fast and conventional characterization technology is important. Future experimental and theoretical studies are required to clarify the following: (i) the type and concentration of the species produced during the gas-phase reactions, (ii) the formation mechanism of amorphous carbon, and (ii) the competitive relationship between the formation of amorphous carbon and few-layer graphene.

Toward large-area ultra-flat graphene films

High roughness is another key issue degrading the performance of SCG, resulting in a decrease in the carrier mobility, mechanical strength, and thermal conductivity.[8,13,77] In contrast with the surface contamination occurring during the high-temperature growth process, the wrinkles or step-bunches [Fig. 3(c)] that increase the roughness are usually formed during the post-growth cooling process because of the large difference in the thermal expansion coefficient between graphene (-7×10^{-6}/K) and the metal substrate (e.g., 16.7×10^{-6}/K for Cu).[1]

Generally, the formation of wrinkles is accompanied by at least three stages of graphene distortion: (i) bending, (ii) detachment from the substrate, and (iii) slipping on the substrate. Therefore, the adhesion energy and friction force of graphene on the metal substrate play crucial roles in the wrinkle-formation process. By performing DFT calculations and MD simulations, two independent studies demonstrated that a strong adhesion force and large frictional force between epitaxial graphene and a Cu(111) substrate enable a compression strain (0.25%–0.4%) to be maintained, which prevent strain release by wrinkle formation.[8,20] Moreover, MD simulation results showed that Stone–Wales defects or grain boundaries can induce the formation of wrinkles.[14] Very recently, using a custom MD simulation package, a complete description of the wrinkle-formation process was developed, including nucleation, propagation, and splitting of the wrinkle on a Cu surface.[78] In contrast, the formation of step bunching is not a result of the release of strain but is driven by the fast diffusion of metal atoms below the step, as well as the reduction in the bending energy of graphene near the step. As proven by a detailed MD simulation, the crystal surface of metal substrates has a significant influence on the formation of step bunching.[79] Thus, more attention should be paid to the vicinal step of metal substrates before growing graphene. In addition, the steps of the metal substrate form a higher step bundle owing to the graphene coating, which releases the local bending energy of graphene. Considering the presence of vicinal steps on the metal surface, avoiding the step bunching during the cooling process is a significant challenge.

GRAPHENE WITH NOVEL PROPERTIES

Generally, the electronic properties of graphene change significantly with the number of layers and stacking order due to interlayer coupling. The conventional stacking order of bilayer graphene (BLG) is the most-stable AB stacking (or Bernal stacking), as shown in the left panel of Fig. 4(a), which results in a zero bandgap.[82,83] When the two layers are stacked with a twisted orientation [right panel, Fig. 4(a)], interesting physical phenomena can occur.[19,21,84–87] For instance, when the twist angle between the two layers of BLG is close to the so-called "magic angle" (~1.1°), the flat band near the Fermi level leads to superconductivity in BLG.[19,21] The twist angle-dependent van Hove singularities (VHSs) in the electronic density of states give rise to the enhanced optical absorption,[88] chiral optical property,[89] and selectively enhanced photocurrent generation.[90,91] The incommensurate BLG with a 30° twist shows quasicrystal ordering with a 12-fold rotational symmetry.[86] However, the controllable growth of BLG with a precise twist angle over large areas continues to face numerous challenges. The growth modes of BLG can be categorized as the wedding cake (WC) or inverted wedding cake (IWC) models according to the stacking sequence, i.e., the second layer of graphene grows above the first layer in the WC structure, while it grows beneath the first layer in the IWC structure [Fig. 4(b)].[80] Based on previous theoretical calculations and experiments, the growth modes can be altered by tuning the concentration of active carbon species or the graphene–substrate interaction.[87,92,93] There have been many reports on the synthesis of bilayer or few-layer graphene films by designing alloy substrates, such as Pt–Si, Cu–Si, and Cu–Ni alloy to effectively tune the carbon solubility of bulk substrates.[14,94,95] However, the precise control of layer number, stacking order, and twist angle of graphene layers is still challenging. The elucidation of the exact growth mechanism by both theoretical and experimental studies is required.

In addition to multilayer graphene, some other structures with novel properties are being investigated. For example, the synthesis of graphene nanoribbons with different edges and widths [Fig. 4(c)] and nitrogen-doped graphene [Fig. 4(d)] is of interest for tailoring the electronic properties.[2,96–98] Although single-crystal narrow graphene nanoribbons and graphitic nitrogen-cluster-doped

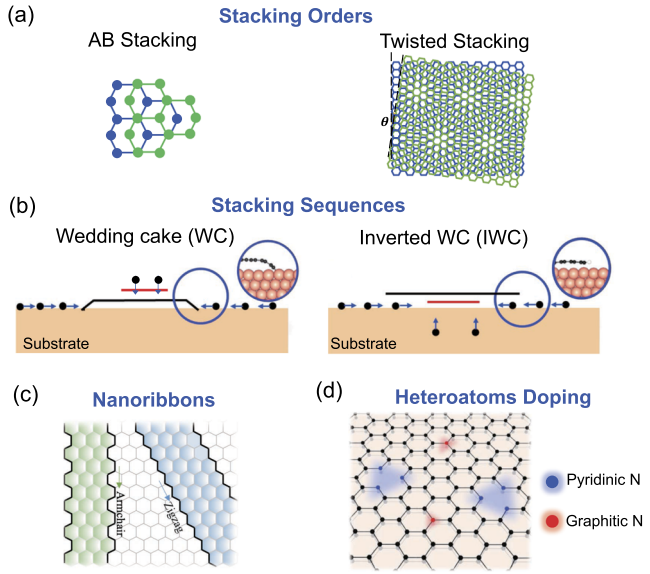

FIG. 4. Approaches for endowing graphene with novel properties. (a) Changing the stacking order of bilayer graphene. Left panel: AB-stacking and right panel: twisted stacking. (b) Different stacking sequences of bilayer graphene: the wedding cake (WC) and inverted wedding cake (IWC) models. Reproduced with permission from Zhang *et al.*, J. Am. Chem. Soc. **136**, 3040 (2014). Copyright 2014 American Chemical Society.[80] Schemes of (c) graphene nanoribbons and (d) N-doped graphene. Reproduced with permission from Lin *et al.*, Sci. Adv. **5**, 8337 (2019). Copyright 2019 The American Association for the Advancement of Science.[81]

graphene have been realized, their controllability are still limited. As a new class of graphene systems, further in-depth exploration of their growth mechanism is required.

CONCLUSIONS AND PERSPECTIVES

The growth of graphene via CVD approaches involves complicated high-temperature reaction processes that cannot be directly observed experimentally. Multiscale theoretical calculations have proved valuable as an effective way to understand the growth mechanism of graphene at the atomic scale to the macroscale, which have greatly contributed to the recent advancements in the CVD growth of graphene films.

With the combination of theoretical and experimental studies, significant success has been achieved in the growth of large SCG on transition-metal substrates. Using a single-seed approach, the size of foot-long graphene on the $Cu_{90}Ni_{10}$ polycrystalline substrate or a growth rate of 200 μm/s has been realized. However, the trade-off between nucleation density and growth rate is a big challenge. Thus, considering the recent breakthrough in the synthesis of single-crystal metal films or foils, we have confident in multi-nuclei approach on single-crystal metal substrates. However, avoiding the imperfect grain boundary of the metal substrate and the small fraction of misaligned graphene domains requires further exploration. To further increase the quality of SCG, much attention should be paid to key issues such as surface contamination, defect density, and roughness. Most importantly, theoretical calculations to provide a deeper understanding of amorphous carbon formation and step-bunching at the vicinal step of the single-crystal metal surface are urgently needed. The novel properties of a new class of graphene-related structures, such as multilayer graphene with various stacking orders, graphene nanoribbons, and heteroatom-doped graphene, have been widely explored theoretically. However, the growth mechanism is still unclear.

For future applications of graphene films, the cost, controllability, and transferability should also be carefully evaluated in the scaling-up production and commercialization. Therefore, technologies such as plasma-enhanced CVD for low-temperature growth, transfer processes or direct growth on target insulating substrates, and industrial CVD system design by CFD simulation deserve to be extensively studied.[15,99–101] In addition, some unknown effects, such as impurities from the solvent or gas phase, can also be carefully considered from a theoretical perspective. We believe that with the rapid development of computational methods and characterization techniques such as *in situ* observation, the preparation and industrialization of graphene materials will continue to make great progress. Moreover, following the success of graphene, theoretical calculations could contribute to the growth of other new two-dimensional materials.

AUTHORS' CONTRIBUTIONS

T.C. and L.Z.S. contributed equally to this work.

ACKNOWLEDGMENTS

This work was financially supported by Beijing National Laboratory for Molecular Science (Grant No. BNLMS-CXTD-202001), the National Natural Science Foundation of China (Grant No. 21773002), the Beijing Municipal Science and Technology Commission (Grant Nos. Z181100004818001, Z191100000819005, and Z201100008720005), and the National Basic Research Program of China (Grant Nos. 2016YFA0200101 and 2016YFA0200103). The author also acknowledges the support from the Institute for Basic Science (Grant No. IBS-R019-D1), South Korea. The High-Performance Computing platform of Peking University is also acknowledged.

DATA AVAILABILITY

The data that support the findings of this study are available from the corresponding authors upon reasonable request.

REFERENCES

[1] L. Sun, G. Yuan, L. Gao, J. Yang, M. Chhowalla, M. H. Gharahcheshmeh, K. K. Gleason, Y. S. Choi, B. H. Hong, and Z. Liu, Nat. Rev. Methods Primers **1**, 5 (2021).
[2] X.-D. Chen, Z. Chen, W.-S. Jiang, C. Zhang, J. Sun, H. Wang, W. Xin, L. Lin, M. K. Priydarshi, H. Yang, Z.-B. Liu, J.-G. Tian, Y. Zhang, Y. Zhang, and Z. Liu, Adv. Mater. **29**, 1603428 (2017).
[3] L. Lin, J. Zhang, H. Su, J. Li, L. Sun, Z. Wang, F. Xu, C. Liu, S. Lopatin, Y. Zhu, K. Jia, S. Chen, D. Rui, J. Sun, R. Xue, P. Gao, N. Kang, Y. Han, H. Q. Xu, Y. Cao, K. S. Novoselov, Z. Tian, B. Ren, H. Peng, and Z. Liu, Nat. Commun. **10**, 1912 (2019).
[4] F. Qing, Y. Hou, R. Stehle, and X. Li, APL Mater. **7**, 020903 (2019).
[5] Y. Hao, M. S. Bharathi, L. Wang, Y. Liu, H. Chen, S. Nie, X. Wang, H. Chou, C. Tan, B. Fallahazad, H. Ramanarayan, C. W. Magnuson, E. Tutuc, B. I. Yakobson, K. F. McCarty, Y.-W. Zhang, P. Kim, J. Hone, L. Colombo, and R. S. Ruoff, Science **342**, 720 (2013).
[6] T. Wu, X. Zhang, Q. Yuan, J. Xue, G. Lu, Z. Liu, H. Wang, H. Wang, F. Ding, Q. Yu, X. Xie, and M. Jiang, Nat. Mater. **15**, 43 (2016).
[7] X. Xu, Z. Zhang, L. Qiu, J. Zhuang, L. Zhang, H. Wang, C. Liao, H. Song, R. Qiao, P. Gao, Z. Hu, L. Liao, Z. Liao, D. Yu, E. Wang, F. Ding, H. Peng, and K. Liu, Nat. Nanotechnol. **11**, 930 (2016).
[8] B. Deng, Z. Pang, S. Chen, X. Li, C. Meng, J. Li, M. Liu, J. Wu, Y. Qi, W. Dang, H. Yang, Y. Zhang, J. Zhang, N. Kang, H. Xu, Q. Fu, X. Qiu, P. Gao, Y. Wei, Z. Liu, and H. Peng, ACS Nano **11**, 12337 (2017).
[9] I. V. Vlassiouk, Y. Stehle, P. R. Pudasaini, R. R. Unocic, P. D. Rack, A. P. Baddorf, I. N. Ivanov, N. V. Lavrik, F. List, N. Gupta, K. V. Bets, B. I. Yakobson, and S. N. Smirnov, Nat. Mater. **17**, 318 (2018).
[10] M. Huang, M. Biswal, H. J. Park, S. Jin, D. Qu, S. Hong, Z. Zhu, L. Qiu, D. Luo, X. Liu, Z. Yang, Z. Liu, Y. Huang, H. Lim, W. J. Yoo, F. Ding, Y. Wang, Z. Lee, and R. S. Ruoff, ACS Nano **12**, 6117 (2018).
[11] B. Deng, Z. Xin, R. Xue, S. Zhang, X. Xu, J. Gao, J. Tang, Y. Qi, Y. Wang, Y. Zhao, L. Sun, H. Wang, K. Liu, M. H. Rummeli, L.-T. Weng, Z. Luo, L. Tong, X. Zhang, C. Xie, Z. Liu, and H. Peng, Sci. Bull. **64**, 659 (2019).
[12] M. Huang and R. S. Ruoff, Acc. Chem. Res. **53**, 800 (2020).
[13] B.-W. Li, D. Luo, L. Zhu, X. Zhang, S. Jin, M. Huang, F. Ding, and R. S. Ruoff, Adv. Mater. **30**, 1706504 (2018).
[14] K. Jia, J. Zhang, L. Lin, Z. Li, J. Gao, L. Sun, R. Xue, J. Li, N. Kang, Z. Luo, M. H. Rummeli, H. Peng, and Z. Liu, J. Am. Chem. Soc. **141**, 7670 (2019).
[15] S. Bae, H. Kim, Y. Lee, X. Xu, J.-S. Park, Y. Zheng, J. Balakrishnan, T. Lei, H. R. Kim, Y. I. Song, Y.-J. Kim, K. S. Kim, B. Özyilmaz, J.-H. Ahn, B. H. Hong, and S. Iijima, Nat. Nanotechnol. **5**, 574 (2010).
[16] J. Zhang, K. Jia, L. Lin, W. Zhao, H. T. Quang, L. Sun, T. Li, Z. Li, X. Liu, L. Zheng, R. Xue, J. Gao, Z. Luo, M. H. Rummeli, Q. Yuan, H. Peng, and Z. Liu, Angew. Chem., Int. Ed. **58**, 14446 (2019).
[17] K. Jia, H. Ci, J. Zhang, Z. Sun, Z. Ma, Y. Zhu, S. Liu, J. Liu, L. Sun, X. Liu, J. Sun, W. Yin, H. Peng, L. Lin, and Z. Liu, Angew. Chem., Int. Ed. **59**, 17214 (2020).
[18] J. M. B. Lopes dos Santos, N. M. R. Peres, and A. H. Castro Neto, Phys. Rev. Lett. **99**, 256802 (2007).
[19] Y. Cao, V. Fatemi, S. Fang, K. Watanabe, T. Taniguchi, E. Kaxiras, and P. Jarillo-Herrero, Nature **556**, 43 (2018).

[20] J. Aprojanz, S. R. Power, P. Bampoulis, S. Roche, A.-P. Jauho, H. J. W. Zandvliet, A. A. Zakharov, and C. Tegenkamp, Nat. Commun. **9**, 4426 (2018).
[21] Y. Cao, D. Chowdhury, D. Rodan-Legrain, O. Rubies-Bigorda, K. Watanabe, T. Taniguchi, T. Senthil, and P. Jarillo-Herrero, Phys. Rev. Lett. **124**, 076801 (2020).
[22] D. Wong, K. P. Nuckolls, M. Oh, B. Lian, Y. Xie, S. Jeon, K. Watanabe, T. Taniguchi, B. A. Bernevig, and A. Yazdani, Nature **582**, 198 (2020).
[23] J. Dong, L. Zhang, and F. Ding, Adv. Mater. **31**, 1801583 (2019).
[24] K. Momeni, Y. Ji, Y. Wang, S. Paul, S. Neshani, D. E. Yilmaz, Y. K. Shin, D. Zhang, J.-W. Jiang, H. S. Park, S. Sinnott, A. van Duin, V. Crespi, and L.-Q. Chen, npj Comput. Mater. **6**, 22 (2020).
[25] J. Gao, Z. Xu, S. Chen, M. S. Bharathi, and Y.-W. Zhang, Adv. Theory Simul. **1**, 1800085 (2018).
[26] T. Cheng, C. Tan, S. Zhang, T. Tu, H. Peng, and Z. Liu, J. Phys. Chem. C **122**, 19970 (2018).
[27] T. Cheng, H. Lang, Z. Li, Z. Liu, and Z. Liu, Phys. Chem. Chem. Phys. **19**, 23942 (2017).
[28] K. Chen, X. Zhou, X. Cheng, R. Qiao, Y. Cheng, C. Liu, Y. Xie, W. Yu, F. Yao, Z. Sun, F. Wang, K. Liu, and Z. Liu, Nat. Photonics **13**, 754 (2019).
[29] Z. Chen, H. Chang, T. Cheng, T. Wei, R. Wang, S. Yang, Z. Dou, B. Liu, S. Zhang, Y. Xie, Z. Liu, Y. Zhang, J. Li, F. Ding, P. Gao, and Z. Liu, Adv. Funct. Mater. **30**, 2001483 (2020).
[30] T. Cheng, L. Sun, Z. Liu, F. Ding, and Z. Liu, Acta Phys.-Chim. Sin. **2020**, 2012006.
[31] T. Cheng, Z. Liu, and Z. Liu, J. Mater. Chem. C **8**, 13819 (2020).
[32] L. H. Thomas, Math. Proc. Cambridge Philos. Soc. **23**, 542 (1927).
[33] P. Hohenberg and W. Kohn, Phys. Rev. **136**, B864 (1964).
[34] W. Kohn and L. J. Sham, Phys. Rev. **140**, A1133 (1965).
[35] J. P. Perdew, Phys. Rev. B **33**, 8822 (1986).
[36] A. D. Becke, Phys. Rev. A **38**, 3098 (1988).
[37] J. Heyd, G. E. Scuseria, and M. Ernzerhof, J. Chem. Phys. **118**, 8207 (2003).
[38] W. Zhang, P. Wu, Z. Li, and J. Yang, J. Phys. Chem. C **115**, 17782 (2011).
[39] X. Wang, Q. Yuan, J. Li, and F. Ding, Nanoscale **9**, 11584 (2017).
[40] H. Shu, X.-M. Tao, and F. Ding, Nanoscale **7**, 1627 (2015).
[41] H. J. C. Berendsen, J. P. M. Postma, W. F. van Gunsteren, A. Dinola, and J. R. Haak, J. Chem. Phys. **81**, 3684 (1984).
[42] K. Chenoweth, A. C. T. van Duin, and W. A. Goddard III, J. Phys. Chem. A **112**, 1040 (2008).
[43] H. M. Aktulga, J. C. Fogarty, S. A. Pandit, and A. Y. Grama, Parallel Comput. **38**, 245 (2012).
[44] Z. Xu, G. Zhao, L. Qiu, X. Zhang, G. Qiao, and F. Ding, npj Comput. Mater. **6**, 14 (2020).
[45] K. Laasonen, A. Pasquarello, R. Car, C. Lee, and D. Vanderbilt, Phys. Rev. B **47**, 010142 (1993).
[46] M. Iannuzzi, A. Laio, and M. Parrinello, Phys. Rev. Lett. **90**, 238302 (2003).
[47] Q. Cui, M. Elstner, E. Kaxiras, T. Frauenheim, and M. Karplus, J. Phys. Chem. B **105**, 569 (2001).
[48] B. Aradi, B. Hourahine, and T. Frauenheim, J. Phys. Chem. A **111**, 5678 (2007).
[49] D. Yin, Z. Qiu, P. Li, and Z. Li, Acta Phys.-Chim. Sin. **34**, 1116 (2018).
[50] M. Gaus, Q. Cui, and M. Elstner, J. Chem. Theory Comput. **7**, 931 (2011).
[51] J. Dong, D. Geng, F. Liu, and F. Ding, Angew. Chem., Int. Ed. **58**, 7723 (2019).
[52] J. Zhuang, W. Zhao, L. Qiu, J. Xin, J. Dong, and F. Ding, J. Phys. Chem. C **123**, 9902 (2019).
[53] J. Zhuang, R. Zhao, J. Dong, T. Yan, and F. Ding, Phys. Chem. Chem. Phys. **18**, 2932 (2016).
[54] P. Li, Z. Li, and J. Yang, J. Phys. Chem. C **121**, 025949 (2017).
[55] P. Wu, H. Jiang, W. Zhang, Z. Li, Z. Hou, and J. Yang, J. Am. Chem. Soc. **134**, 6045 (2012).
[56] X. Kong, J. Zhuang, L. Zhu, and F. Ding, npj Comput. Mater. **7**, 14 (2021).
[57] X. Zeng, Z. Qiu, P. Li, Z. Li, and J. Yang, CCS Chem. **2**, 460 (2020).
[58] Z. Li, W. Zhang, X. Fan, P. Wu, C. Zeng, Z. Li, X. Zhai, J. Yang, and J. Hou, J. Phys. Chem. C **116**, 010557 (2012).
[59] G. Li, S.-H. Huang, and Z. Li, Phys. Chem. Chem. Phys. **17**, 022832 (2015).
[60] J. Gao and F. Ding, Angew. Chem., Int. Ed. **53**, 14031 (2014).
[61] Y. Wang, A. J. Page, Y. Nishimoto, H.-J. Qian, K. Morokuma, and S. Irle, J. Am. Chem. Soc. **133**, 18837 (2011).
[62] J. Zhang, L. Lin, K. Jia, L. Sun, H. Peng, and Z. Liu, Adv. Mater. **32**, 1903266 (2020).
[63] X. Zhang, Z. Xu, L. Hui, J. Xin, and F. Ding, J. Phys. Chem. Lett. **3**, 2822 (2012).
[64] C. Liu, X. Xu, L. Qiu, M. Wu, R. Qiao, L. Wang, J. Wang, J. Niu, J. Liang, X. Zhou, Z. Zhang, M. Peng, P. Gao, W. Wang, X. Bai, D. Ma, Y. Jiang, X. Wu, D. Yu, E. Wang, J. Xiong, F. Ding, and K. Liu, Nat. Chem. **11**, 730 (2019).
[65] Y. Xie, T. Cheng, C. Liu, K. Chen, Y. Cheng, Z. Chen, L. Qiu, G. Cui, Y. Yu, L. Cui, M. Zhang, J. Zhang, F. Ding, K. Liu, and Z. Liu, ACS Nano **13**, 010272 (2019).
[66] Q. Yuan, B. I. Yakobson, and F. Ding, J. Phys. Chem. Lett. **5**, 3093 (2014).
[67] X. Zhang, T. Wu, Q. Jiang, H. Wang, H. Zhu, Z. Chen, R. Jiang, T. Niu, Z. Li, Y. Zhang, Z. Qiu, G. Yu, A. Li, S. Qiao, H. Wang, Q. Yu, and X. Xie, Small **15**, 1805395 (2019).
[68] S. Jin, M. Huang, Y. Kwon, L. Zhang, B.-W. Li, S. Oh, J. Dong, D. Luo, M. Biswal, B. V. Cunning, P. V. Bakharev, I. Moon, W. J. Yoo, D. C. Camacho-Mojica, Y.-J. Kim, S. H. Lee, B. Wang, W. K. Seong, M. Saxena, F. Ding, H.-J. Shin, and R. S. Ruoff, Science **362**, 1021 (2018).
[69] M. Wu, Z. Zhang, X. Xu, Z. Zhang, Y. Duan, J. Dong, R. Qiao, S. You, L. Wang, J. Qi, D. Zou, N. Shang, Y. Yang, H. Li, L. Zhu, J. Sun, H. Yu, P. Gao, X. Bai, Y. Jiang, Z.-J. Wang, F. Ding, D. Yu, E. Wang, and K. Liu, Nature **581**, 406 (2020).
[70] B. Deng, Z. Liu, and H. Peng, Adv. Mater. **31**, 1800996 (2019).
[71] S. Chen, J. Gao, B. M. Srinivasan, and Y.-W. Zhang, Acta Phys.-Chim. Sin. **35**, 1119 (2019).
[72] J. Dong, L. Zhang, X. Dai, and F. Ding, Nat. Commun. **11**, 5862 (2020).
[73] Y. Li, L. Sun, H. Liu, Y. Wang, and Z. Liu, Inorg. Chem. Front. **8**, 182 (2020).
[74] L. Sun, L. Lin, Z. Wang, D. Rui, Z. Yu, J. Zhang, Y. Li, X. Liu, K. Jia, K. Wang, L. Zheng, B. Deng, T. Ma, N. Kang, H. Xu, K. S. Novoselov, H. Peng, and Z. Liu, Adv. Mater. **31**, 1902978 (2019).
[75] J. Zhang, L. Sun, K. Jia, X. Liu, T. Cheng, H. Peng, L. Lin, and Z. Liu, ACS Nano **14**, 10796 (2020).
[76] L. Zheng, Y. Chen, N. Li, J. Zhang, N. Liu, J. Liu, W. Dang, B. Deng, Y. Li, X. Gao, C. Tan, Z. Yang, S. Xu, M. Wang, H. Yang, L. Sun, Y. Cui, X. Wei, P. Gao, H.-W. Wang, and H. Peng, Nat. Commun. **11**, 8 (2020).
[77] G. H. Han, F. Güneş, J. J. Bae, E. S. Kim, S. J. Chae, H.-J. Shin, J.-Y. Choi, D. Pribat, and Y. H. Lee, Nano Lett. **11**, 4144 (2011).
[78] C. Zhao, F. Liu, X. Kong, T. Yan, and F. Ding, Int. J. Smart Nano Mater. **11**, 277 (2020).
[79] D. Yi, D. Luo, Z.-J. Wang, J. Dong, X. Zhang, M.-G. Willinger, R. S. Ruoff, and F. Ding, Phys. Rev. Lett. **120**, 246101 (2018).
[80] X. Zhang, L. Wang, J. Xin, B. I. Yakobson, and F. Ding, J. Am. Chem. Soc. **136**, 3040 (2014).
[81] L. Lin, J. Li, Q. Yuan, Q. Li, J. Zhang, L. Sun, D. Rui, Z. Chen, K. Jia, M. Wang, Y. Zhang, M. H. Rummeli, N. Kang, H. Q. Xu, F. Ding, H. Peng, and Z. Liu, Sci. Adv. **5**, 8337 (2019).
[82] Y. Zhang, T.-T. Tang, C. Girit, Z. Hao, M. C. Martin, A. Zettl, M. F. Crommie, Y. R. Shen, and F. Wang, Nature **459**, 820 (2009).
[83] T. Ohta, A. Bostwick, T. Seyller, K. Horn, and E. Rotenberg, Science **313**, 951 (2006).
[84] W. Yan, M. Liu, R.-F. Dou, L. Meng, L. Feng, Z.-D. Chu, Y. Zhang, Z. Liu, J.-C. Nie, and L. He, Phys. Rev. Lett. **109**, 126801 (2012).
[85] G. Li, A. Luican, J. M. B. Lopes dos Santos, A. H. Castro Neto, A. Reina, J. Kong, and E. Y. Andrei, Nat. Phys. **6**, 109 (2010).
[86] W. Yao, E. Wang, C. Bao, Y. Zhang, K. Zhang, K. Bao, C. K. Chan, C. Chen, J. Avila, M. C. Asensio, J. Zhu, and S. Zhou, Proc. Natl. Acad. Sci. U.S.A. **115**, 6928 (2018).
[87] L. Sun, Z. Wang, Y. Wang, L. Zhao, Y. Li, B. Chen, S. Huang, S. Zhang, W. Wang, D. Pei, H. Fang, S. Zhong, H. Liu, J. Zhang, L. Tong, Y. Chen, Z. Li, M. H. Rümmeli, K. S. Novoselov, H. Peng, L. Lin, and Z. Liu, Nat. Commun. **12**, 2391 (2021).
[88] P. Moon and M. Koshino, Phys. Rev. B **87**, 205404 (2013).
[89] C.-J. Kim, A. Sánchez-Castillo, Z. Ziegler, Y. Ogawa, C. Noguez, and J. Park, Nat. Nanotechnol. **11**, 520 (2016).

[90]J. Yin, H. Wang, H. Peng, Z. Tan, L. Liao, L. Lin, X. Sun, A. L. Koh, Y. Chen, H. Peng, and Z. Liu, Nat. Commun. **7**, 010699 (2016).
[91]Z. Tan, J. Yin, C. Chen, H. Wang, L. Lin, L. Sun, J. Wu, X. Sun, H. Yang, Y. Chen, H. Peng, and Z. Liu, ACS Nano **10**, 6725 (2016).
[92]H. Q. Ta, D. J. Perello, D. L. Duong, G. H. Han, S. Gorantla, V. L. Nguyen, A. Bachmatiuk, S. V. Rotkin, Y. H. Lee, and M. H. Rümmeli, Nano Lett. **16**, 6403 (2016).
[93]I. Vlassiouk, M. Regmi, P. Fulvio, S. Dai, P. Datskos, G. Eres, and S. Smirnov, ACS Nano **5**, 6069 (2011).
[94]Y. Li, L. Sun, H. Liu, Y. Wang, and Z. Liu, Catalysts **10**, 1305 (2020).
[95]V. L. Nguyen, D. L. Duong, S. H. Lee, J. Avila, G. Han, Y.-M. Kim, M. C. Asensio, S.-Y. Jeong, and Y. H. Lee, Nat. Nanotechnol. **15**, 861 (2020).
[96]J. Wang, R. Van Pottelberge, A. Jacobs, B. Van Duppen, and F. M. Peeters, Phys. Rev. B **103**, 035426 (2021).
[97]H. S. Wang, L. Chen, K. Elibol, L. He, H. Wang, C. Chen, C. Jiang, C. Li, T. Wu, C. X. Cong, T. J. Pennycook, G. Argentero, D. Zhang, K. Watanabe, T. Taniguchi, W. Wei, Q. Yuan, J. C. Meyer, and X. Xie, Nat. Mater. **20**, 202 (2021).
[98]S. Bu, N. Yao, M. A. Hunter, D. J. Searles, and Q. Yuan, npj Comput. Mater. **6**, 128 (2020).
[99]D. Wei, Y. Lu, C. Han, T. Niu, W. Chen, and A. T. S. Wee, Angew. Chem., Int. Ed. **52**, 014121 (2013).
[100]Z. Chen, X. Zhang, Z. Dou, T. Wei, Z. Liu, Y. Qi, H. Ci, Y. Wang, Y. Li, H. Chang, J. Yan, S. Yang, Y. Zhang, J. Wang, P. Gao, J. Li, and Z. Liu, Adv. Mater. **30**, 1801608 (2018).
[101]T. Cheng, Z. Liu, Z. Liu, and F. Ding, ACS Nano **15**, 7399 (2021).